Since January 2020 Elsevier has created a COVID-19 resource centre with free information in English and Mandarin on the novel coronavirus COVID-19. The COVID-19 resource centre is hosted on Elsevier Connect, the company's public news and information website.

Elsevier hereby grants permission to make all its COVID-19-related research that is available on the COVID-19 resource centre - including this research content - immediately available in PubMed Central and other publicly funded repositories, such as the WHO COVID database with rights for unrestricted research re-use and analyses in any form or by any means with acknowledgement of the original source. These permissions are granted for free by Elsevier for as long as the COVID-19 resource centre remains active.

Life Sciences 280 (2021) 119752

Contents lists available at ScienceDirect

Life Sciences

journal homepage: www.elsevier.com/locate/lifescie

# Zinc supplementation augments the suppressive effects of repurposed NF-κB inhibitors on ACE2 expression in human lung cell lines

Ming-Cheng Lee [a], Yin-Kai Chen [b,c], Jyy-Jih Tsai-Wu [d], Yih-Jen Hsu [e], Bor-Ru Lin [a,e,*]

[a] Department of Internal Medicine, Hospital and College of Medicine, National Taiwan University, Taipei 10051, Taiwan, ROC
[b] Graduate Institute of Clinical Medicine, College of Medicine, National Taiwan University, Taipei 10002, Taiwan, ROC
[c] Department of Hematology, National Taiwan University Cancer Center, Taipei 10672, Taiwan, ROC
[d] Department of Medical Research, National Taiwan University Hospital, Taipei 10051, Taiwan, ROC
[e] Department of Integrated Diagnostics and Therapeutics, National Taiwan University Hospital, Taipei 10051, Taiwan, ROC

ARTICLE INFO

*Keywords:*
ACE2
NF-kappa B
ROS
Triclabendazole
Emetine
Zinc

ABSTRACT

*Aims:* Angiotensin-converting enzyme 2 (ACE2) is a key negative regulator of the renin-angiotensin system and also a major receptor for severe acute respiratory syndrome coronavirus 2 (SARS-CoV-2) infection. Here, we reveal a role for NF-κB in human lung cell expression of ACE2, and we further explore the potential utility of repurposing NF-κB inhibitors to downregulate ACE2.

*Main methods:* Expression of ACE2 was assessed by Western blotting and RT-qPCR in multiple human lung cell lines with or without NF-κB inhibitor treatment. Surface ACE2 expression and intracellular reactive oxygen species (ROS) levels were measured with flow cytometry. p50 was knocked down with siRNA. Cytotoxicity was monitored by PARP cleavage and MTS assay.

*Key findings:* Pyrrolidine dithiocarbamate (PDTC), an NF-κB inhibitor, suppressed endogenous ACE2 mRNA and protein expression in H322M and Calu-3 cells. The ROS level in H322M cells was increased after PDTC treatment, and pretreatment with *N*-acetyl-cysteine (NAC) reversed PDTC-induced ACE2 suppression. Meanwhile, treatment with hydrogen peroxide augmented ACE2 suppression in H322M cells with p50 knockdown. Two repurposed NF-κB inhibitors, the anthelmintic drug triclabendazole and the antiprotozoal drug emetine, also reduced ACE2 mRNA and protein levels. Moreover, zinc supplementation augmented the suppressive effects of triclabendazole and emetine on ACE2 expression in H322M and Calu-3 cells.

*Significance:* These results suggest that ACE2 expression is modulated by ROS and NF-κB signaling in human lung cells, and the combination of zinc with triclabendazole or emetine shows promise for clinical treatment of ACE2-related disease.

## 1. Introduction

Angiotensin-converting enzyme 2 (ACE2) has long been known as a negative regulator of the renin-angiotensin system, mainly due to its actions of converting Angiotensin I (Ang I) into Ang 1–9 and Angiotensin II (Ang II) into Ang 1–7 [1]. Based on this function, previous studies in animal models of human diseases have revealed a critical protective role for ACE2 in fibrosis and inflammation of kidney and lung, as well as heart diseases [2–6]. Besides its function as a key regulator of the renin-angiotensin system, ACE2 has also been shown to act as the receptor for three coronaviruses, including HCoV-NL63, SARS-CoV, and the COVID-19-causing virus, SARS-CoV-2 [7]. Preventing the binding of virus to ACE2 is one of the most promising strategies for mitigating infection of these viruses [8,9].

A previous study using *ACE2* knockout mice to model human nephropathy showed that enhanced renal fibrosis and inflammation were largely attributable to marked increases in the intrarenal Ang II signaling and NF-κB signaling pathways [2]. Moreover, work on an animal model of pulmonary fibrosis revealed that upregulation of the ACE2/Ang-(1–7)/Mas axis can protect against pulmonary fibrosis by inhibiting the NF-κB pathway *in vivo*. Additionally, Ang-(1–7) was shown to inhibit angiotensin II induced NF-κB signaling in human fetal lung cells *in vitro* [3]. Intriguingly, angiotensin II was also shown to induce the expression of ACE2 in human cardiac fibroblasts [10], however, the underlying signaling pathway is still unclear. Based on the findings of these previous studies, we suspected that NF-κB signaling

* Corresponding author at: National Taiwan University Hospital, No. 7, Chung-Shan S. Rd., Taipei 10002, Taiwan, ROC.
*E-mail address:* brucelin@ntuh.gov.tw (B.-R. Lin).

https://doi.org/10.1016/j.lfs.2021.119752
Received 19 February 2021; Received in revised form 6 June 2021; Accepted 14 June 2021
Available online 23 June 2021
0024-3205/© 2021 The Authors. Published by Elsevier Inc. This is an open access article under the CC BY-NC-ND license (http://creativecommons.org/licenses/by-nc-nd/4.0/).

might play a regulatory role in ACE2 expression.

Viral spike proteins or dsRNA of SARS-CoV-2 may activate the NF-κB pathway in non-immune cells such as alveolar epithelial cells and endothelial cells, eventually leading to a cytokine storm that is associated with severe COVID-19 [11,12]. Therefore, inhibition of the NF-κB pathway has been considered to be a potential therapeutic strategy for alleviating severe COVID-19. Abnormal NF-κB signaling is also linked with certain neoplasias, and Miller et al. identified several drugs with previously unappreciated effects on NF-κB signaling that may have anticancer effects [13]. Among the drugs, the antiprotozoal drug emetine and anthelmintic drug triclabendazole were shown to inhibit NF-κB signaling *via* inhibition of IκBα phosphorylation. Since antiprotozoal and anthelmintic drugs generally have lower cellular toxicities than anti-cancer drugs, we elected to investigate the effects of emetine and triclabendazole on ACE2 expression in this study.

Zinc is widely known to mediate antiviral effects [14]. Observational studies have reported that low baseline zinc levels in hospitalized adults were associated with poor outcomes following SARS-CoV-2 infection [15], suggesting a potential benefit from zinc supplementation in reducing COVID-19 morbidity and mortality. Because zinc supplements are cost-efficient, globally available, simple to use, and have little to no side effects, the treatment has a great potential for combination with other repurposed drugs to combat viral infection.

In the study, we found that ACE2 expression in lung cell lines is regulated by ROS and NF-κB signaling, and it can be suppressed by treating with zinc in combination with triclabendazole or emetine.

## 2. Materials and methods

### 2.1. Reagents

Pyrrolidine dithiocarbamate (PDTC, 548000; Merck Millipore), triclabendazole (HY-B0621; MCE) and emetine dihydrochloride (HY-B1479A, MCE) were dissolved in dimethyl sulfoxide (DMSO), whereas $ZnSO4{\cdot}7H_2O$ (zinc sulfate heptahydrate, Z0501; Sigma-Aldrich) and N-acetyl-L-cysteine (NAC, A9165; Sigma-Aldrich) were dissolved in ddH2O. An equal concentration of solvent was routinely used to treat the control group in the experiments.

### 2.2. Cell culture

Lung cancer cells A549, H322M, H460 and H522 were cultured in Roswell Park Memorial Institute (RPMI) 1640 medium, and H1299 cells were cultured in Dulbecco's modified Eagle's medium (DMEM). Calu-3 cells were kindly provided by Dr. Tsung-Tao Huang (National Applied Research Laboratories, Hsinchu, Taiwan) and were cultured in Minimum Essential Medium (α-MEM) (Gibco BRL). All culture media were supplemented with 10% heat-inactivated fetal bovine serum and 1% penicillin/streptomycin solution (Gibco-BRL). The cells were grown in a humidified incubator containing 5% $CO_2$ at 37 °C.

### 2.3. Cell viability

H322M or Calu-3 cells were seeded in 96-well plates overnight and treated for 48 h with different concentrations of PDTC (12.5–200 μM), triclabendazole (12.5–200 μM), emetine (31.2–500 nM) or DMSO as a vehicle control. The cell viability was then evaluated by the MTS assay. Twenty microliters of MTS reagent (Promega Corporation, Madison, WI, USA) was added to each well. After 1 h of incubation at 37 °C, the absorbance of each well was measured at 490 nm using an EPOCH2 microplate reader (BioTek Instruments, USA).

### 2.4. Real-time quantitative RT-PCR (qRT-PCR)

Total RNA was isolated using the PureLink® RNA Mini Kit (Ambion by Life Technologies) according to the manufacturer's instructions. One microgram of total RNA was used to synthesize the cDNA, using IQ2 MMLV RT-Script (Bio-Genesis) with Oligo-dT primer (Gene Teks). Quantitative PCR was performed using Kapa SYBR fast qPCR master mix (Kapa Biosystems, Woburn, MA, USA). The primer sequences were GAPDH-fw: 5′-GAAGGTGAAGGTCGGAGT-3′ and GAPDH-rev: 5′-GAAGATGGTGATGGGATTTC-3′; ACE2-fw: 5′-GGACCCAGGAAATGTTCAGA-3′ and ACE2-rev: 5′-GGCTGCAGAAAGTGACATGA-3′. The qPCR reaction was run in a final volume of 20 μL, including 1 μL of reverse transcriptase product, 10 μL of 2× Kapa SYBR fast qPCR master mix, and 0.6 μL of each primer (10 μM). The qPCR mixtures were pre-incubated at 95 °C for 3 min, followed by 40 cycles of 95 °C for 3 s and 60 °C for 30 s. All qPCR measurements were performed in triplicates on a CFX Connect™ Real-Time System (Bio-Rad Laboratories, Inc.).

### 2.5. Western blot

The cells were dissolved in lysis buffer containing 50 mM Tris-HCl (pH 7.4), 150 mM NaCl, 0.25% deoxycholic acid, 1% NP-40, 1 mM EDTA, and protease inhibitor Cocktail Set III (Calbiochem). Fifty micrograms of protein were fractionated *via* 10% SDS-PAGE and transferred to Immobilon Transfer Membranes (Millipore). Primary antibodies used in this study included those against β-actin (GTX109639; dilution 1:10,000; GeneTex), poly (ADP-ribose) polymerase (PARP) (9542S; dilution 1:1000; Cell Signaling Technology), ACE2 (bs-1004R; dilution 1:1000; Bioss), p65 (SC-8008; dilution 1:1000; Santa Cruz Biotechnology), p50 (SC-8414; dilution 1:1000; Santa Cruz Biotechnology) and GAPDH (GTX100118; dilution 1:1000; GeneTex). HRP-conjugated secondary antibodies recognizing mouse-IgG (7076) or rabbit-IgG (7074) were purchased from Cell Signaling Technology and used at dilutions of 1:5000–10,000. The chemiluminescence signal was captured on a BioSpectrum 810 Imaging System with VisionWorks software (UVP).

### 2.6. Flow cytometry

Caul-3 cells were treated with PDTC (100 μM) or DMSO control for 48 h. Then, cells were detached using phosphate-buffered saline (PBS, pH 7.4) with 5 mM EDTA. Cells were then blocked with 10% FBS for 30 min on ice and subsequently probed with non-immune mouse IgG or mouse anti-ACE2 (sc-390,851; Santa Cruz Biotechnology; dilution 1:100) for 1 h on ice. Then, Alexa Fluor 488-conjugated donkey anti-mouse IgG (Invitrogen; dilution 1:500) was added and samples were incubated for 30 min on ice. The samples were analyzed with Becton-Dickinson FACSVerse Flow Cytometer.

### 2.7. Detection of ROS using CellROX® deep red

H322M cells were seeded in 6-well plates, and treated with NAC (5 mM) or PDTC (100 μM) for 24 h, or cells were pretreated with NAC for 30 min followed by PDTC for 24 h. Treatment with $H_2O_2$ for 30 min served as a positive control. The cells were stained using the Cellular Reactive Oxygen Species Detection Assay Kit (Deep Red Fluorescence, ab186029; Abcam) according to the manufacturer's instructions, and analyzed with a Becton-Dickinson FACSVerse Flow Cytometer.

### 2.8. Nuclear–cytoplasmic fractionation

Nuclear–cytoplasmic fractionation was conducted using the NE-PER Nuclear and Cytoplasmic Extraction Reagents kit (Thermo Fisher Scientific) according to the manufacturer's protocol.

### 2.9. Knockdown of p50 by siRNA

Scrambled control and SMARTpool siRNA targeting p50 (Dharmacon) were electroporated into H322M cells using the Neon transfection system (Invitrogen) according to the manufacturer's instructions. Forty-

eight hours after electroporation, the knockdown efficiencies were determined according to the protein levels of the target genes using Western blot assay.

### 2.10. Statistical analysis

Results are expressed as mean ± SD. Prism 6.0 software (GraphPad) was used to perform statistical tests. Student's *t*-test was performed for experiments with two groups. Differences between multiple groups were analyzed by one-way ANOVA followed by *post hoc* analysis using Tukey's multiple comparisons test. $P < 0.05$ was considered to be significant for all experiments.

## 3. Results

### 3.1. PDTC decreases endogenous ACE2 expressions in H322M and Calu-3 cells

To begin exploring the regulatory mechanisms of ACE2 expression in lung cells, we first evaluated the endogenous protein levels of ACE2 in

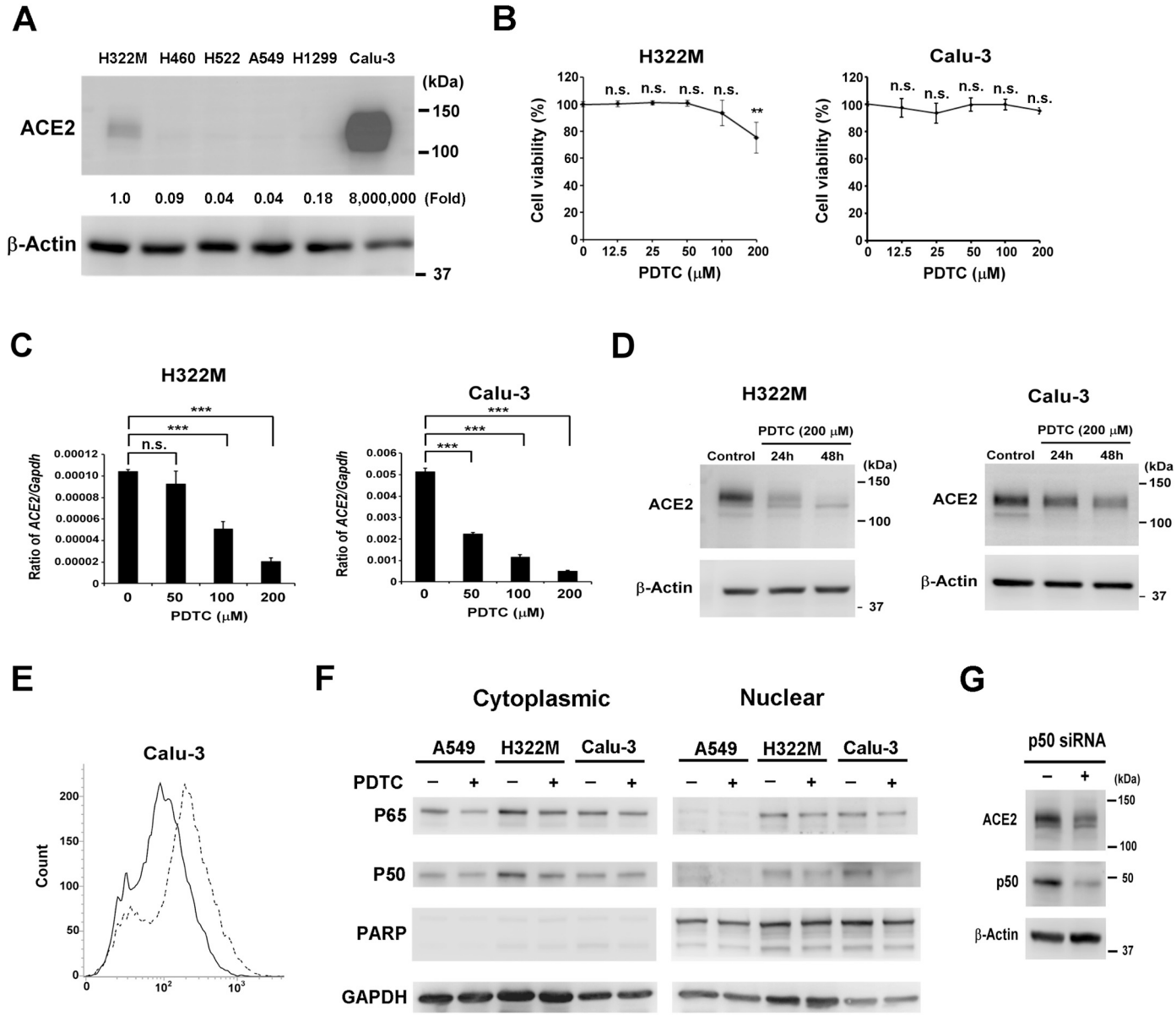


**Fig. 1.** PDTC treatment inhibits endogenous ACE2 expressions in H322M and Calu-3 lung cancer cells. (A) The endogenous ACE2 protein levels in six different lung cancer cells were measured by Western blot with β-actin as a loading control. The intensity of the bands was measured by VisionWorks software (UVP). Fold change relative to control was calculated using ACE2: β-actin ratio. (B) H322M and Calu-3 cells were seeded in 96-well plates and treated with various concentrations of PDTC (0, 12.5, 25, 50, 100 or 200 μM) for 48 h. Then, the relative cell viabilities were determined by MTS assay. Error bars represent the standard deviation. The viability of control cells was taken as 100%, and the other groups are reported as percent of the control. (n.s. indicates non-significance, and $^{**}P < 0.005$.) (C) H322M and Calu-3 cells were treated with various concentrations of PDTC (0, 50, 100 or 200 μM) for 24 h, and RNA was isolated for *ACE2* measurement by real-time qRT-PCR. The data were normalized to *GAPDH*. Error bars represent the mean ± SD (n = 3). ($^{***}P < 0.0005$; and n.s. indicates non-significance.) (D) H322M and Calu-3 cells were treated with 200 μM PDTC, and protein was harvested at different time points for Western blot analysis of ACE2; β-actin was used as a loading control. (E) Calu-3 cells were treated with 100 μM PDTC (solid line) or DMSO (dashed line) for 48 h, and cells were subjected to a flow cytometry assay to measure ACE2 protein on the cell surface. (F) A549, H322M and Calu-3 cells were treated with or without 200 μM PDTC for 24 h, and cytoplasmic and nuclear fractions were prepared for Western blotting to detect changes in nuclear localization of NF-κB subunits, p65 and p50. (G) H322M cells were electroporated with control or p50 siRNA. After 48 h, the cells were lysed for Western blot analysis of ACE2 and p50; β-actin was used as a loading control.

six human lung cell lines. We found that ACE2 protein was detectable in Calu-3 and H322M cells, with especially abundant ACE2 expression observed in Calu-3 cells (Fig. 1A). Therefore, Calu-3 and H322M cells were used in subsequent experiments. To test whether NF-κB pathway affects ACE2 expression, an inhibitor of NF-κB (PDTC) was used to treat cells *in vitro*. Dose up to 200 μM PDTC did not induce abundant cell death in either cell types (Fig. 1B). To determine the effect of PDTC on *ACE2* mRNA expression, both H322M and Calu-3 cells were treated with various concentrations of the drug. We found that PDTC treatment decreased the RNA levels of *ACE2* in a dose-dependent manner (Fig. 1C). In addition, the effect of PDTC on ACE2 protein level was also examined, and we found that PDTC treatment obviously decreased ACE2 protein level in a time-dependent manner in both H322M and Calu-3 cells (Fig. 1D). Furthermore, ACE2 levels on the cell surface of Calu-3 cells were assessed using flow cytometry. We found that cell-surface ACE2 was decreased in PDTC-treated Calu-3 cells (Fig. 1E). To further assess the association between ACE2 expression and NF-κB activity, the subcellular distributions of the p65 and p50 subunits of NF-κB were monitored by Western blotting of H322M and Calu-3 cells, as well as A549 cells in which ACE2 is undetectable. We found that both p65 and p50 subunits were readily found in cytoplasmic and nuclear fractions of H322M and Calu-3 cells, whereas both p65 and p50 were mainly detected in cytoplasmic fractions of A549 cells (Fig. 1F). In addition, the nuclear localization of p50 was decreased in H322M and Calu-3 cells treated with PDTC. These findings suggest that NF-κB signaling is associated with endogenous ACE2 expression in lung cell lines. Notably, however, when the p50 subunit of NF-κB was knocked down with siRNA, ACE2 expression was not obviously suppressed in H322M cells (Fig. 1G), suggesting that an alternative mechanism for PDTC-induced ACE2 suppression could exist.

### 3.2. NAC reverses PDTC-derived ACE2 suppression in H322M cells

PDTC is a thiol compound that exerts both pro-oxidant and antioxidant effects [16]. To explore whether ROS is involved in PDTC-derived ACE2 suppression, ROS levels were assessed by flow cytometry in H322M cells treated with NAC or PDTC alone, or a combination of the two. We found that NAC treatment reduced the ROS level, whereas PDTC treatment increased the ROS level in H322M cells, as compared with untreated control cells. Moreover, NAC pretreatment prevented PDTC-induced ROS accumulation (Fig. 2A). In addition, *ACE2* mRNA and protein expression were evaluated in H322M cells after the same treatments. We found that NAC treatment enhanced *ACE2* mRNA and protein expression, and NAC pretreatment prevented PDTC-induced ACE2 suppression (Fig. 2B and C), suggesting PDTC acts as a pro-oxidant in H322M cells. To mimic the pro-oxidant activity of PDTC, H322M cells with p50 knockdown were treated with $H_{2O2}$, and ACE2 expression was evaluated. Immunoblotting of PARP was conducted to monitor potential apoptotic cell death. We found that $H_{2O2}$ treatment enhanced ACE2 suppression in p50-silenced H322M cells, compared with the p50-silenced cells (Fig. 2D). These results suggest that NF-κB inhibition and ROS induction are involved in PDTC-induced suppression of ACE2 in H322M cells.

### 3.3. Triclabendazole and emetine suppress endogenous ACE2 expression in H322M cells

Drug repurposing is a fast approach of using clinically approved drugs for treatment of different diseases, bypassing many steps of the long drug discovery process. Based on this idea, two NF-κB inhibitors, triclabendazole and emetine [13], were selected for further investigations into their ability to modulate ACE2 expression in lung cell lines. First, the cytotoxic effects of triclabendazole and emetine were evaluated in H322M cells to identify an appropriate range of concentrations for further experiments. We found that treatments up to 100 μM triclabendazole and 125 nM emetine treatment did not overtly inhibit cell growth (Fig. 3A). Thus, H322M cells were treated with triclabendazole or emetine, and *ACE2* expression was measured. We found that treatment of 100 μM triclabendazole or 100 nM emetine could inhibit *ACE2* mRNA expression (Fig. 3B). Furthermore, the treatments decreased ACE2 protein expression in a time-dependent manner (Fig. 3C). Immunoblotting of PARP was conducted to monitor apoptotic cell death; appreciable levels of cleaved PARP, a marker of apoptosis, were only detected in cells with triclabendazole treatment for 48 h. In addition, we found that NAC pretreatment reversed 50 μM triclabendazole or 100 nM emetine-induced ACE2 suppression (Fig. 3D). These findings suggest that triclabendazole and emetine act similar to PDTC in order to suppress ACE2 expression in H322M cells.

### 3.4. Zinc supplementation augments the suppressive effects of triclabendazole and emetine on ACE2 expressions in H322M and Calu-3 cells

In combination therapy, different drugs may be used to simultaneously modulate similar molecular pathways and increase treatment efficacy while reducing the doses and side effects of toxic drugs. Zinc is a trace element with potent immunoregulatory and antiviral properties, so we wanted to test its potential for use in combination with NF-κB inhibitors. Therefore, we first investigated the cytotoxic and ACE2 modulatory effects of zinc sulfate on H322M cells and found that *ACE2* mRNA and protein expression were not obviously affected by treatments of 100 to 300 μM zinc sulfate. At these doses, no cleaved PARP was detected either (Fig. 4A and B). To further explore whether zinc can augment the ACE2 suppressive effects of triclabendazole and emetine, H322M and Calu-3 cells were treated with triclabendazole, emetine, or zinc sulfate alone, or the combination of zinc sulfate and triclabendazole or emetine. We found that ACE2 expression was not dramatically repressed in H322M and Calu-3 cells after 24 h treatment of triclabendazole, emetine, or zinc sulfate alone, whereas the combined treatment of zinc sulfate with triclabendazole or emetine clearly suppressed ACE2 protein expression (Fig. 4C and D). Meanwhile, no apparent cleavage of PARP was detected after any treatment. These findings indicate that the combined treatment of zinc sulfate with triclabendazole or emetine is more effective than monotreatment at suppressing ACE2 expression in human lung cells.

## 4. Discussion

ACE2 is widely expressed in lung and other cardiovascular tissues, in addition to gut, kidney, adipose tissue and the central nervous system, but overall expression of *ACE2* is rather low in the lung [5,17]. Notably, single-cell RNA sequencing experiments revealed that *ACE2* expression in lung is heterogenous among cell types, as the gene is mainly expressed in lung ciliated cells with lower expression in alveolar type 2 cells [17,18]. Similarly, previous studies delineating ACE2 protein distribution in lung cell cultures indicated that ACE2 protein can be detected in the human adenocarcinoma cell line, Calu-3, but it is undetectable in primary human airway epithelial and type II alveolar epithelial cells, the human bronchial epithelial cell (HBEC)-6KT line, and the type II alveolar epithelial cell line, A549. Thus, expression of ACE2 protein is absent or low in airway and alveolar epithelial cells of human lungs, and it is likely that a mechanism exists to dynamically regulate ACE2 expression [19].

In this present study, we found that among our panel of six different lung cell lines, endogenous ACE2 protein expression could only be detected in Calu-3 and H322M cells (Fig. 1A). Calu-3 cells showed the most abundant ACE2 expression, consistent with previous findings [19]. Notably, the Calu-3 cell line was derived from human bronchial epithelium and comprises a submucosal gland cell type with cilia-like microvilli [20]. The abundant ACE2 expression in Calu-3 cells is therefore in accordance with a previous study that showed the *ACE2* gene is highly expressed in lung ciliated cells [18]. In addition, the single-cell

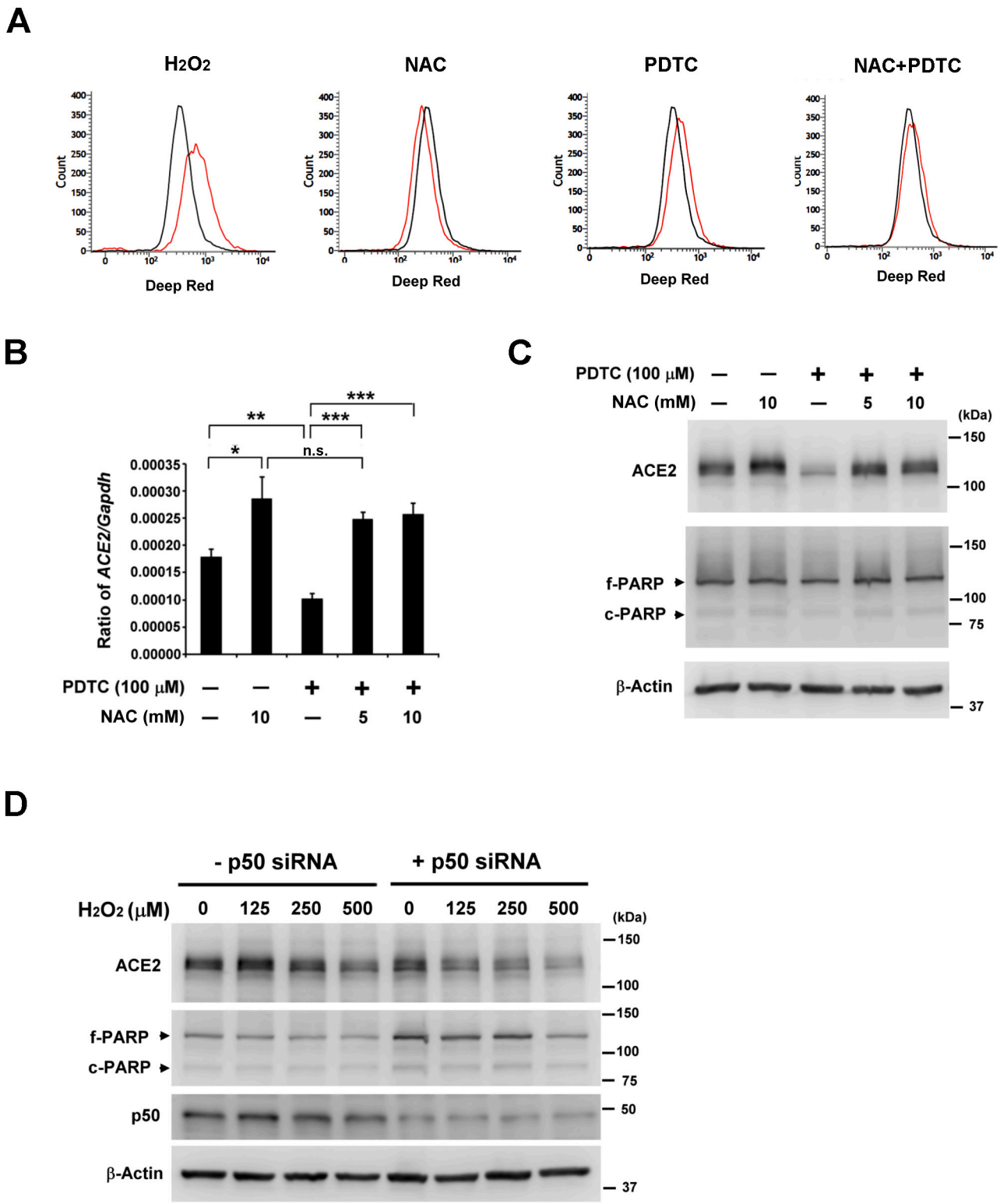


**Fig. 2.** Thiol antioxidant NAC blocks PDTC-induced suppression of ACE2 in H322M cells. (A) H322M cells were treated without (black line) or with (red line) 5 mM NAC or 200 μM PDTC alone or in combination for 24 h. Then, cells were stained using the Cellular ROS assay kit (deep red). Intracellular ROS levels were analyzed with a Becton-Dickinson FACSVerse Flow Cytometer. Cells treated with $H_2O_2$ for 30 min as a positive control. (B) H322M cells, with or without NAC pretreatment for 30 min, were treated with PDTC for 24 h. Total RNA was collected for *ACE2* measurement by real-time qRT-PCR. The data were normalized to *GAPDH*. Error bars represent the mean ± SD (n = 3). (*$P < 0.05$, ** $P < 0.005$, ***$P < 0.0005$, and n.s. indicates non-significance.) (C) The treated cells were lysed for Western blot analysis of ACE2 and PARP; β-actin was used as a loading control. The bands indicating full-length PARP (f-PARP) and the cleaved fragment (c-PARP) are indicated. (D) H322M cells were electroporated with control or p50 siRNA for 24 h, and then, cells were treated with $H_2O_2$ for an additional 24 h. The treated cells were lysed for Western blot analysis of ACE2, p50 and PARP; β-actin was used as a loading control. (For interpretation of the references to color in this figure legend, the reader is referred to the web version of this article.)

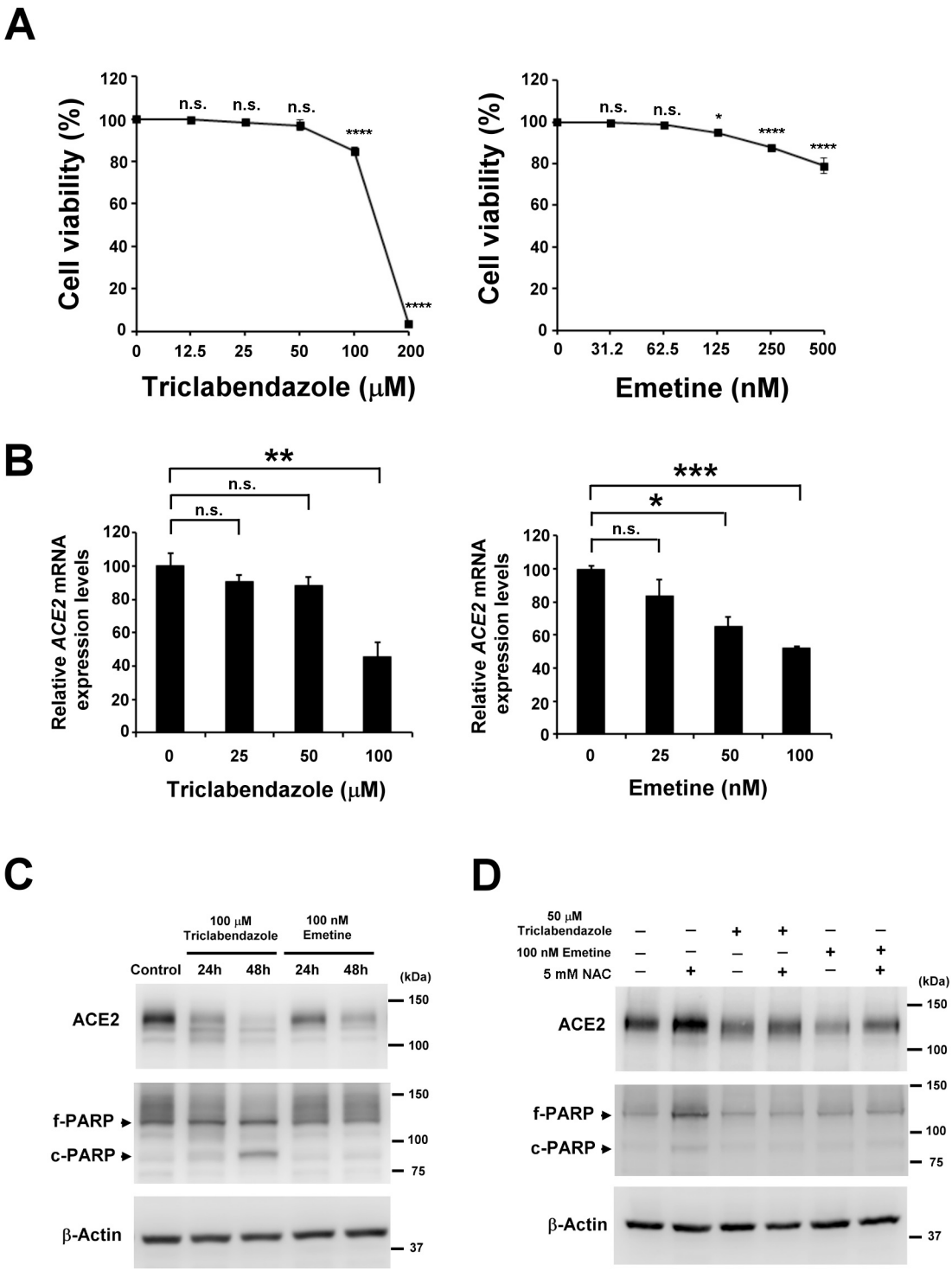


**Fig. 3.** Clinically approved drugs, triclabendazole and emetine, suppress endogenous ACE2 expression in H322M cells. (A) H322M cells were seeded in 96-well plates and treated with various concentrations of triclabendazole (0, 12.5, 25, 50, 100 or 200 μM) or emetine (0, 31.2, 62.5, 125, 250, or 500 nM) for 48 h. Then, the relative cell viabilities were determined by MTS assay. Error bars represent the standard deviation. The viability of control cells was designated as 100%, and the viabilities of other groups are expressed as percent of the control. (n.s. indicates non-significance, *P < 0.05, and ****P < 0.0001.) (B) H322M cells were treated with various concentrations of triclabendazole (0, 50, or 100 μM) or emetine (0, 50, or 100 nM) for 24 h, and total RNA was collected for *ACE2* measurement by real-time qRT-PCR. The data were normalized to *GAPDH*. Error bars represent the mean ± SD (n = 3). (*P < 0.05, **P < 0.005, ***P < 0.0005, and n.s. indicates non-significance.) (C) H322M cells were treated with 100 μM triclabendazole or 100 nM emetine. Total protein was harvested at different time points for Western blot analysis of ACE2 and PARP; β-actin was used as a loading control. (D) H322M cells were pretreated with NAC or vehicle for 30 min, and subsequently treated with triclabendazole (50 μM) or emetine (100 nM) for 48 h. The treated cells were lysed for Western blot analysis of ACE2 and PARP; β-actin was used as a loading control. The bands for full-length PARP (f-PARP) and the cleaved fragment (c-PARP) are indicated.

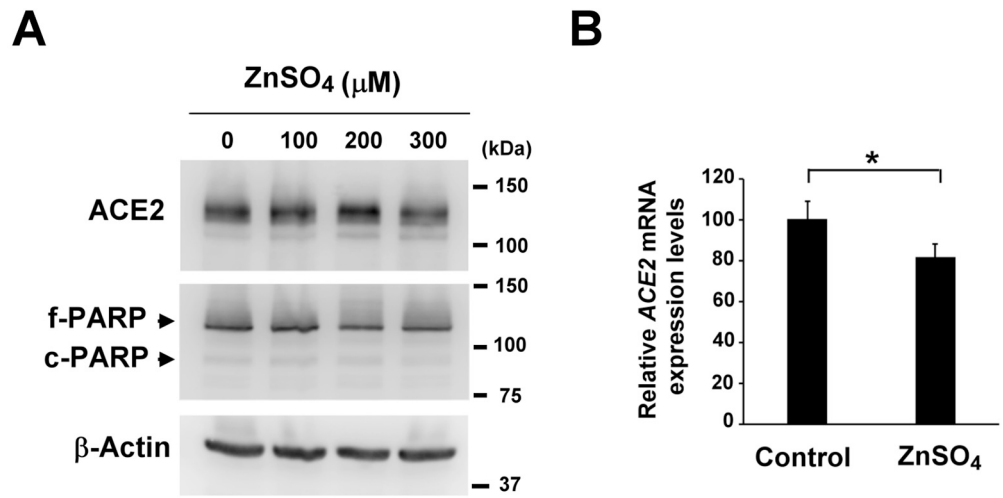


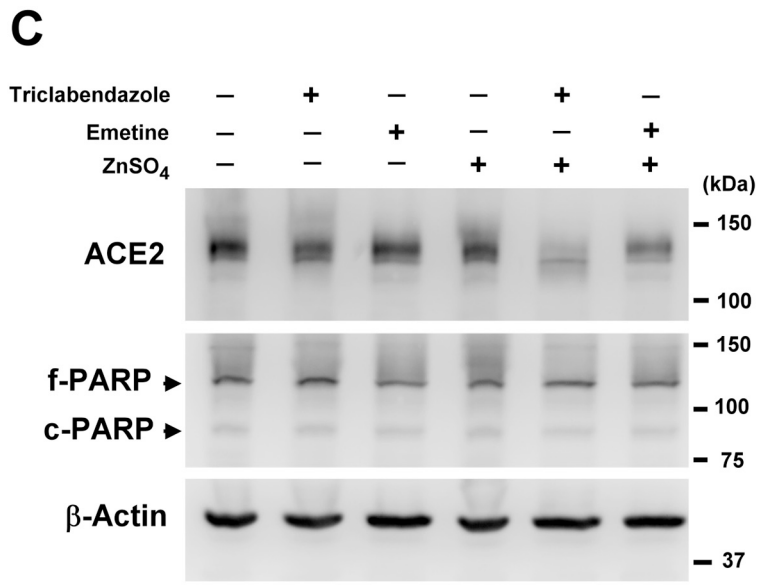


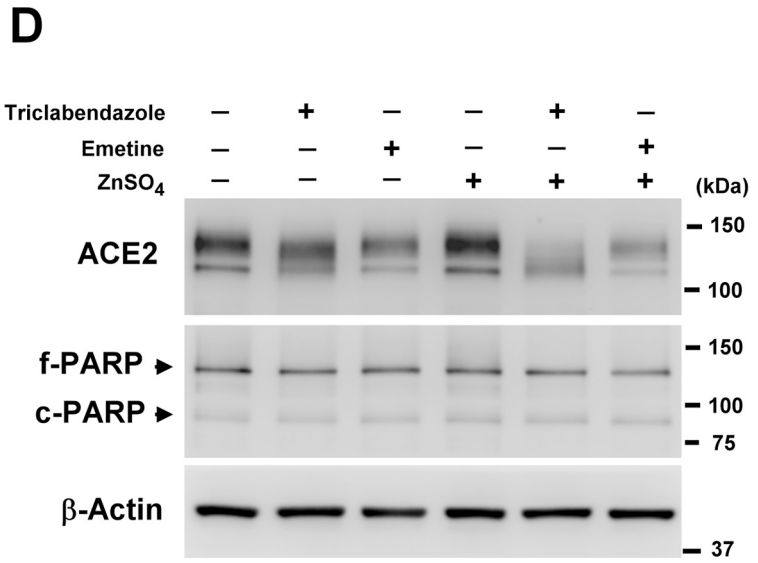


**Fig. 4.** Zinc sulfate and NF-κB inhibitors cooperatively suppress ACE2 expression in H322M and Calu-3 cells. (A) H322M cells were treated with various concentrations of zinc sulfate (0, 100, 200 or 300 μM) for 48 h, followed by lysis for Western blot analysis of ACE2 and PARP; β-actin was used as a loading control. (B) H322M cells were treated with zinc sulfate (300 μM) for 24 h, and total RNA was collected for *ACE2* measurement by real-time qRT-PCR. The data were normalized to *GAPDH*. Error bars represent the mean ± SD (n = 3). (*P < 0.05.) (C) H322M cells and (D) Calu-3 cells were treated with triclabendazole (50 μM), emetine (100 nM), zinc sulfate (150 μM) alone, or in combination with zinc sulfate (150 μM) and triclabendazole or emetine for 24 h. Treated cells were lysed for Western blot analysis of ACE2 and PARP; β-actin was used as a loading control. The bands for full-length PARP (f-PARP) and the cleaved fragment (c-PARP) are indicated.

RNA sequencing study indicated that *ACE2* is expressed at low levels in the alveolar cluster of organoid-derived bronchioalveolar-like cultures [21]. This finding is in accordance with our observation of relatively low but detectable ACE2 protein levels in H322M cells, which were derived from a primary bronchioalveolar carcinoma of the lung [22]. Based on this low but detectable expression level, we considered H322M to be a preferred cell model for investigations of both positive and negative regulators of ACE2 expression in the lung.

The overactivation of the Ang II/AT1R axis is associated with NF-κB-dependent inflammation and disease [23]. ACE2 can prevent the detrimental effects of Ang II/AT1R axis by directly catalyzing Ang II, as well as indirectly inhibiting NF-κB singling through its activation of the Ang(1–7)/MasR axis [3,5,24]. A previous study indicated that Ang II can induce ACE2 expression in human cardiofibroblasts [10], however, whether NF-κB signaling is involved in the regulating ACE2 expression in those cells remains to be seen. Here, we showed that administration of PDTC, an NF-κB inhibitor, downregulated endogenous *ACE2* mRNA and protein expression in Calu-3 and H322M cells in a dose- and time-dependent manner (Fig. 1C and D), suggesting that NF-κB signaling is required for ACE2 expression in lung cells. A wide variety of common human malignancies exhibit constitutive activation of NF-κB, including pancreatic cancer, lung, cervical, prostate, breast and gastric carcinoma [25]. Here, we found that NF-κB subunits p65 and p50 could be detected in both cytoplasmic and nuclear fractions of H322M and Calu-3 cells, whereas the subunits were mostly only detected in the cytoplasmic fractions in A549 cells (Fig. 1F), suggesting that H322M and Calu-3 cells exhibit constitutive NF-κB activation along with endogenous ACE2 expression.

When using p50-targeted siRNA to block NF-κB signaling, we observed that ACE2 expression was not dramatically repressed in H322M cells (Fig. 1G), suggesting that PDTC-derived NF-κB inhibition may cooperate with other events in PDTC-induced ACE2 suppression in H322M cells. PDTC is a metal-chelating compound that exerts both pro-oxidant and antioxidant effects [16]. Here, we found that PDTC treatment enhanced the ROS levels of H322M cells, and pretreatment with the thiol-containing antioxidant, NAC reversed the effect (Fig. 2A). Thus, PDTC appears to act as a pro-oxidant in H322M cells. Furthermore, NAC pretreatment reversed PDTC-induced ACE2 suppression at both mRNA and protein levels (Fig. 2B and C), which is in accordance with the results of a previous study that showed thiol antioxidants can reverse PDTC-mediated attenuation of NF-κB DNA binding activity [26]. Moreover, the administration of hydrogen peroxide augmented ACE2 inhibition in H322M cells with p50 silencing (Fig. 2D). This observation is consistent with the previous finding that pretreatment of buthionine sulfoximine, which induces oxidative stress in cells by irreversibly inhibiting γ-glutamylcysteine synthetase, greatly enhanced the suppressive effect of PDTC on NF-κB activity [26]. These findings suggest that ROS increases and NF-κB inhibition may be involved in PDTC-induced suppression of ACE2. However, PDTC is a pleiotropic compound with actions that include metal-chelation, reduction of cellular glutathione content, action as a copper and zinc ionophore, and inhibition of NF-κB activity [26]. Therefore, we cannot rule out the possibility that other effects of PDTC, besides NF-κB inhibition and ROS increases, may also play a role in mediating PDTC-induced ACE2 suppression.

Currently, a number of repurposed drugs known to interrupt the virus life cycle or modulate of host immune response are being investigated in clinical trials to treat moderate-to-severe COVID-19 [27]. The identification of FDA-approved drugs that have potential to effectively control SARS-CoV-2 infection is urgently needed. To better position our findings for translation to clinical application, the antiprotozoal drug emetine and anthelmintic drug triclabendazole were utilized to inhibit NF-κB and suppress ACE2 expression. The IC50 values of emetine and triclabendazole are respectively 0.31 μM and 25.1 μM for inhibiting IκBα phosphorylation [13] and administration of 100 nM emetine or 100 μM triclabendazole significantly repressed ACE2 expression at the mRNA and protein levels of H322M cells (Fig. 3B and C). It is noteworthy that the serum levels of inflammatory cytokines were shown to be significantly reduced by emetine treatment in a pulmonary hypertension rat model [28]. Moreover, triclabendazole treatment obviously reduced inflammatory cytokine levels in patients with acute or chronic fasciolosis, indicating improved immunological response [29]. The present *in vitro* results and earlier *in vivo* studies suggest that emetine and triclabendazole may have therapeutic potential for COVID-19 patients. The drugs are expected to act by limiting cellular accessibility to the virus and modulating host immune response. Of course, our findings in cell culture must be further extended to physiological models and clinical evaluation before any conclusions about efficacy can be made.

Combination therapies have proven successful in a variety of medical areas, such as infectious and metabolic diseases. The advantages of combination therapy include increased treatment efficacy, reduced dose and side effects of toxic drugs, prevention of acquired drug resistance, and reduced duration of treatment. Previous studies showed that zinc may exert anti-coronavirus and anti-inflammatory effects through inhibition of SARS-CoV RNA polymerase and disruption of NF-κB signaling, respectively [30,31]. Moreover, zinc sulfate may mimic PDTC actions, such as NF-κB inhibition [26]. Notably, 57.4% of COVID-19 patients were found to be zinc deficient, and the patients with deficient zinc levels had higher rates of complications, acute respiratory distress syndrome, prolonged hospital stay, and increased mortality [15]. Despite a paucity of direct clinical data, previous findings suggest that modulation of zinc status may be beneficial in COVID-19. In this study, we found that ACE2 expression was suppressed after a 24 h-treatment with the combination of 150 μM zinc sulfate and 50 μM triclabendazole or 100 nM emetine in H322M and Calu-3 cells (Fig. 4C and D), and the suppression was stronger than that resulting from mono-treatment of triclabendazole or emetine. Taken together, these findings suggest that zinc supplementation may augment the inhibitory effect of triclabendazole and emetine on ACE2 expression. Given that ACE2 has multiple physiological roles in regulating cardiovascular, renal and innate immune systems, targeting ACE2 for disease treatment requires careful consideration of the potential positive and negative effects on the patient [32].

## 5. Conclusions

In the present study, we show that ACE2 expression is regulated by ROS and NF-κB signaling in human lung cell line. In addition, we found that triclabendazole and emetine, two FDA-approved drugs known to inhibit NF-κB, also suppressed ACE2 expression. Moreover, zinc supplementation enhanced the suppressive effects of these two drugs. Therefore, we suggest that the combination treatment of zinc with triclabendazole or emetine should be considered for clinical treatment of ACE2-related diseases, such as COVID-19.

## Declaration of competing interest

The authors declare no competing interests.

*Acknowledgments*

We thank the staff of the Second Core Lab, Department of Medical Research, National Taiwan University Hospital for technical support during the study. We also thank the "Liver Disease Prevention & Treatment Research Foundation, Taiwan" for partial funding support.

*Funding*

This study was financially supported partly from NTUH grants (1) NTUH 99S-1309, (2) NTUH 101-S1867, (3) 107-14, and (4) 108-13, and partly from the National Science Council of the Republic of China grants (1) NSC 98-2314-B-002-091-MY3 and (2) NSC 101-2320-B-002-010-

MY3.

## References


[1] T. Behl, I. Kaur, S. Bungau, A. Kumar, M.S. Uddin, C. Kumar, G. Pal, Sahil, K. Shrivastava, G. Zengin, The dual impact of ACE2 in COVID-19 and ironical actions in geriatrics and pediatrics with possible therapeutic solutions, Life Sci. 257 (2020), 118075, https://doi.org/10.1016/j.lfs.2020.118075.

[2] Z. Liu, X.R. Huang, H.Y. Chen, J.M. Penninger, H.Y. Lan, Loss of angiotensin-converting enzyme 2 enhances TGF-beta/Smad-mediated renal fibrosis and NF-kappaB-driven renal inflammation in a mouse model of obstructive nephropathy, Lab. Investig. 92 (2012) 650–661, https://doi.org/10.1038/labinvest.2012.2.

[3] Y. Meng, C.H. Yu, W. Li, T. Li, W. Luo, S. Huang, P.S. Wu, S.X. Cai, X. Li, Angiotensin-converting enzyme 2/angiotensin-(1–7)/Mas axis protects against lung fibrosis by inhibiting the MAPK/NF-kappaB pathway, Am. J. Respir. Cell Mol. Biol. 50 (2014) 723–736, https://doi.org/10.1165/rcmb.2012-0451OC.

[4] J. Zhong, R. Basu, D. Guo, F.L. Chow, S. Byrns, M. Schuster, H. Loibner, X.H. Wang, J.M. Penninger, Z. Kassiri, et al., Angiotensin-converting enzyme 2 suppresses pathological hypertrophy, myocardial fibrosis, and cardiac dysfunction, Circulation 122 (2010) 717–728, https://doi.org/10.1161/CIRCULATIONAHA.110.955369, 718 p following 728.

[5] M. Gheblawi, K. Wang, A. Viveiros, Q. Nguyen, J.C. Zhong, A.J. Turner, M. K. Raizada, M.B. Grant, G.Y. Oudit, Angiotensin-converting enzyme 2: SARS-CoV-2 receptor and regulator of the renin-angiotensin system: celebrating the 20th anniversary of the discovery of ACE2, Circ. Res. 126 (2020) 1456–1474, https://doi.org/10.1161/CIRCRESAHA.120.317015.

[6] N. Banu, S.S. Panikar, L.R. Leal, A.R. Leal, Protective role of ACE2 and its downregulation in SARS-CoV-2 infection leading to macrophage activation syndrome: therapeutic implications, Life Sci. 256 (2020), 117905, https://doi.org/10.1016/j.lfs.2020.117905.

[7] M. Hasoksuz, S. Kilic, F. Sarac, Coronaviruses and SARS-COV-2, Turk. J. Med. Sci. 50 (2020) 549–556, https://doi.org/10.3906/sag-2004-127.

[8] J. Lu, Y. Hou, S. Ge, X. Wang, J. Wang, T. Hu, Y. Lv, H. He, C. Wang, Screened antipsychotic drugs inhibit SARS-CoV-2 binding with ACE2 in vitro, Life Sci. 266 (2021), 118889, https://doi.org/10.1016/j.lfs.2020.118889.

[9] C.G. Benitez-Cardoza, J.L. Vique-Sanchez, Potential inhibitors of the interaction between ACE2 and SARS-CoV-2 (RBD), to develop a drug, Life Sci. 256 (2020), 117970, https://doi.org/10.1016/j.lfs.2020.117970.

[10] T.C. Kuan, T.H. Yang, C.H. Wen, M.Y. Chen, I.L. Lee, C.S. Lin, Identifying the regulatory element for human angiotensin-converting enzyme 2 (ACE2) expression in human cardiofibroblasts, Peptides 32 (2011) 1832–1839, https://doi.org/10.1016/j.peptides.2011.08.009.

[11] A. Hariharan, A.R. Hakeem, S. Radhakrishnan, M.S. Reddy, M. Rela, The role and therapeutic potential of NF-kappa-B pathway in severe COVID-19 patients, Inflammopharmacology (2020), https://doi.org/10.1007/s10787-020-00773-9.

[12] A. Jafarzadeh, P. Chauhan, B. Saha, S. Jafarzadeh, M. Nemati, Contribution of monocytes and macrophages to the local tissue inflammation and cytokine storm in COVID-19: lessons from SARS and MERS, and potential therapeutic interventions, Life Sci. 257 (2020), 118102, https://doi.org/10.1016/j.lfs.2020.118102.

[13] S.C. Miller, R. Huang, S. Sakamuru, S.J. Shukla, M.S. Attene-Ramos, P. Shinn, D. Van Leer, W. Leister, C.P. Austin, M. Xia, Identification of known drugs that act as inhibitors of NF-kappaB signaling and their mechanism of action, Biochem. Pharmacol. 79 (2010) 1272–1280, https://doi.org/10.1016/j.bcp.2009.12.021.

[14] I. Wessels, B. Rolles, L. Rink, The potential impact of Zinc supplementation on COVID-19 pathogenesis, Front. Immunol. 11 (2020) 1712, https://doi.org/10.3389/fimmu.2020.01712.

[15] D. Jothimani, E. Kailasam, S. Danielraj, B. Nallathambi, H. Ramachandran, P. Sekar, S. Manoharan, V. Ramani, G. Narasimhan, I. Kaliamoorthy, et al., COVID-19: poor outcomes in patients with zinc deficiency, Int. J. Infect. Dis. 100 (2020) 343–349, https://doi.org/10.1016/j.ijid.2020.09.014.

[16] C.H. Kim, J.H. Kim, C.Y. Hsu, Y.S. Ahn, Zinc is required in pyrrolidine dithiocarbamate inhibition of NF-kappaB activation, FEBS Lett. 449 (1999) 28–32, https://doi.org/10.1016/s0014-5793(99)00390-7.

[17] F. Qi, S. Qian, S. Zhang, Z. Zhang, Single cell RNA sequencing of 13 human tissues identify cell types and receptors of human coronaviruses, Biochem. Biophys. Res. Commun. 526 (2020) 135–140, https://doi.org/10.1016/j.bbrc.2020.03.044.

[18] W. Sungnak, N. Huang, C. Becavin, M. Berg, R. Queen, M. Litvinukova, C. Talavera-Lopez, H. Maatz, D. Reichart, F. Sampaziotis, et al., SARS-CoV-2 entry factors are highly expressed in nasal epithelial cells together with innate immune genes, Nat. Med. 26 (2020) 681–687, https://doi.org/10.1038/s41591-020-0868-6.

[19] J.A. Aguiar, B.J. Tremblay, M.J. Mansfield, O. Woody, B. Lobb, A. Banerjee, A. Chandiramohan, N. Tiessen, Q. Cao, A. Dvorkin-Gheva, et al., Gene expression and in situ protein profiling of candidate SARS-CoV-2 receptors in human airway epithelial cells and lung tissue, Eur. Respir. J. 56 (2020), https://doi.org/10.1183/13993003.01123-2020.

[20] T. Furubayashi, D. Inoue, N. Nishiyama, A. Tanaka, R. Yutani, S. Kimura, H. Katsumi, A. Yamamoto, T. Sakane, Comparison of various cell lines and three-dimensional mucociliary tissue model systems to estimate drug permeability using an in vitro transport study to predict nasal drug absorption in Rats, Pharmaceutics 12 (2020), https://doi.org/10.3390/pharmaceutics12010079.

[21] M.M. Lamers, J. van der Vaart, K. Knoops, S. Riesebosch, T.I. Breugem, A. Z. Mykytyn, J. Beumer, D. Schipper, K. Bezstarosti, C.D. Koopman, et al., An organoid-derived bronchioalveolar model for SARS-CoV-2 infection of human alveolar type II-like cells, EMBO J. 40 (2021), e105912, https://doi.org/10.15252/embj.2020105912.

[22] S. Sei, J.K. Mussio, Q.E. Yang, K. Nagashima, R.E. Parchment, M.C. Coffey, R. H. Shoemaker, J.E. Tomaszewski, Synergistic antitumor activity of oncolytic reovirus and chemotherapeutic agents in non-small cell lung cancer cells, Mol. Cancer 8 (2009) 47, https://doi.org/10.1186/1476-4598-8-47.

[23] Y. Meng, T. Li, G.S. Zhou, Y. Chen, C.H. Yu, M.X. Pang, W. Li, Y. Li, W.Y. Zhang, X. Li, The angiotensin-converting enzyme 2/angiotensin (1–7)/Mas axis protects against lung fibroblast migration and lung fibrosis by inhibiting the NOX4-derived ROS-mediated RhoA/Rho kinase pathway, Antioxid. Redox Signal. 22 (2015) 241–258, https://doi.org/10.1089/ars.2013.5818.

[24] X. Yu, L. Cui, F. Hou, X. Liu, Y. Wang, Y. Wen, C. Chi, C. Li, R. Liu, C. Yin, Angiotensin-converting enzyme 2-angiotensin (1–7)-Mas axis prevents pancreatic acinar cell inflammatory response via inhibition of the p38 mitogen-activated protein kinase/nuclear factor-kappaB pathway, Int. J. Mol. Med. 41 (2018) 409–420, https://doi.org/10.3892/ijmm.2017.3252.

[25] R.R. Rasmi, K.M. Sakthivel, C. Guruvayoorappan, NF-kappaB inhibitors in treatment and prevention of lung cancer, Biomed. Pharmacother. 130 (2020), 110569, https://doi.org/10.1016/j.biopha.2020.110569.

[26] C.H. Kim, J.H. Kim, J. Lee, C.Y. Hsu, Y.S. Ahn, Thiol antioxidant reversal of pyrrolidine dithiocarbamate-induced reciprocal regulation of AP-1 and NF-kappaB, Biol. Chem. 384 (2003) 143–150, https://doi.org/10.1515/BC.2003.015.

[27] A. Pandey, A.N. Nikam, A.B. Shreya, S.P. Mutalik, D. Gopalan, S. Kulkarni, B. S. Padya, G. Fernandes, S. Mutalik, R. Prassl, Potential therapeutic targets for combating SARS-CoV-2: drug repurposing, clinical trials and recent advancements, Life Sci. 256 (2020), 117883, https://doi.org/10.1016/j.lfs.2020.117883.

[28] M.A.H. Siddique, K. Satoh, R. Kurosawa, N. Kikuchi, M. Elias-Al-Mamun, J. Omura, T. Satoh, M. Nogi, S. Sunamura, S. Miyata, et al., Identification of emetine as a therapeutic agent for pulmonary arterial hypertension: novel effects of an old drug, Arterioscler. Thromb. Vasc. Biol. 39 (2019) 2367–2385, https://doi.org/10.1161/ATVBAHA.119.313309.

[29] A.F. Allam, M.M. Osman, M.H. El-Sayed, S.R. Demian, IL-1, IL-4 production and IgE levels in acute and chronic fasciolosis before and after triclabendazole treatment, J. Egypt. Soc. Parasitol. 30 (2000) 781–790.

[30] A.V. Skalny, L. Rink, O.P. Ajsuvakova, M. Aschner, V.A. Gritsenko, S.I. Alekseenko, A.A. Svistunov, D. Petrakis, D.A. Spandidos, J. Aaseth, et al., Zinc and respiratory tract infections: perspectives for COVID19 (Review), Int. J. Mol. Med. 46 (2020) 17–26, https://doi.org/10.3892/ijmm.2020.4575.

[31] A.J. te Velthuis, S.H. van den Worm, A.C. Sims, R.S. Baric, E.J. Snijder, M.J. van Hemert, Zn(2) inhibits coronavirus and arterivirus RNA polymerase activity in vitro and zinc ionophores block the replication of these viruses in cell culture, PLoS Pathog. 6 (2010), e1001176, https://doi.org/10.1371/journal.ppat.1001176.

[32] H. Jia, E. Neptune, H. Cui, Targeting ACE2 for COVID-19 therapy: opportunities and challenges, Am. J. Respir. Cell Mol. Biol. 64 (2021) 416–425, https://doi.org/10.1165/rcmb.2020-0322PS.